

Contribution from the Department of Chemistry, University of Florence, Via G. Capponi 7, 50121 Florence, Italy,  
 Institute of Agricultural Chemistry, Faculty of Agricultural Sciences, University of Bologna, Bologna, Italy,  
 IBM T. J. Watson Research Center, Yorktown Heights, New York, New York 10598,  
 and Department of Molecular Biophysics and Biochemistry, Yale University School of Medicine,  
 333 Cedar Street, New Haven, Connecticut 06510

## Copper(II) as a Probe of the Active Centers of Alkaline Phosphatase

Ivano Bertini,<sup>\*1a</sup> Claudio Luchinat,<sup>1a,b</sup> Maria Silvia Viezzoli,<sup>1a</sup> Lucia Banci,<sup>1a</sup> Seymour H. Koenig,<sup>1c</sup>  
 Helios T. Leung,<sup>1d</sup> and Joseph E. Coleman<sup>1d</sup>

Received March 24, 1988

Alkaline phosphatase (AP) contains three metal ion binding sites at each active center A, B, and C, forming a triangle of 3.9, 4.9, and 7 Å between the three metal ions. Water  $^1\text{H } T_1^{-1}$  of solutions of metal-free apoalkaline phosphatase and of derivatives containing 1, 2, 3, and 4 mol of Cu(II)/mol of enzyme dimer have been measured between 0.01 and 40 MHz (NMRD). Two Cu(II) ions added to the apoenzyme sequentially occupy the A sites at both pH 6 and pH 8, giving rise to NMRD typical of Cu(II) coordinated to exchangeable water molecules and bound to isolated sites in macromolecules. A d-d absorption maximum at 690 nm ( $\epsilon/\text{Cu(II)} = 145 \text{ M}^{-1} \text{ cm}^{-1}$ ) and an axially symmetric ESR signal ( $g_{\parallel} = 2.32$ ,  $g_{\perp} = 2.09$ ,  $A_{\parallel} = 164 \times 10^{-4} \text{ cm}^{-1}$ ) show the Cu(II) ions in the Cu<sub>2</sub>AP to occupy identical sites. The third and fourth equivalents of Cu(II) added to the enzyme result in the quenching of the relaxivity of the Cu<sub>2</sub>E<sub>2</sub>AP (E for "empty") as well as a loss of the room-temperature ESR signal. Magnetic susceptibility measurements (room temperature) show that there is strong antiferromagnetic coupling between the Cu(II) ions in the A and B sites ( $J \approx 120 \text{ cm}^{-1}$ ). Part of the loss of the relaxivity on the binding of the second pair of Cu(II) ions to alkaline phosphatase can be attributed to the magnetic interaction between the Cu(II) ions at sites A and B. This interaction may reflect the presence of a bridging ligand between Cu<sub>A</sub> and Cu<sub>B</sub>, either OH<sup>-</sup> or Ser-O<sup>-</sup>. <sup>31</sup>P NMR shows that phosphate binds to only one monomer of Cu<sub>2</sub>E<sub>2</sub>AP; i.e., phosphate binding is negatively cooperative. Phosphate binding is accompanied by a time-dependent shift in the d-d transitions to give two absorption maxima, one at the original 690 nm and a new one at 790 nm. Simultaneously, the room-temperature ESR spectrum decreases in amplitude and the paramagnetic component of the water proton relaxation rate decreases. These findings suggest that phosphate binding to Cu<sub>2</sub>E<sub>2</sub>AP induces the migration of Cu(II) from the A site of the phosphate-free monomer to the B site of the phospho monomer. These data are analyzed in terms of the water and ligand structure at the active centers of the Cu(II) derivatives of alkaline phosphatase.

### Introduction

Alkaline phosphatase (AP)<sup>2</sup> from *Escherichia coli* is a dimer of identical subunits, each of MW 47 000 (429 amino acids).<sup>3,4</sup> Each monomer contains three metal ion binding sites, designated A, B, and C.<sup>3-14</sup> The crystal structure of alkaline phosphatase containing six Cd(II) ions has shown that the A and B sites are 3.9 Å apart, although no bridging ligand has been identified in the Zn(II) or Cd(II) enzymes.<sup>14</sup> Site C is 4.9 Å from the B site. The hydroxyl group of Ser-102, the residue that forms the phosphoserine intermediate (E-P)<sup>2</sup> in the reaction pathway during phosphomonoester hydrolysis, is located between metal sites A

and B and is slightly to one side of the axis connecting them.<sup>14</sup> The seryl hydroxyl appears closer to the B-site Zn(II) ion but cannot definitely be said to be ligated to this metal ion from the current electron density maps.<sup>14</sup> In all probability the B-site metal ion activates the seryl hydroxyl by favoring the formation of Ser-O<sup>-</sup>.<sup>4,14</sup>

In the presence of excess zinc and magnesium, the A and B sites are occupied by Zn(II), while Mg(II) binds to the C site.<sup>14</sup> In the absence of other metal ions, Mg(II) will bind to both the B and C sites but has no affinity for the A sites.<sup>4</sup> The order of metal ion binding to alkaline phosphatase has been investigated in some detail. In the pH range 6-7, Cu(II) and Co(II)<sup>15-21</sup> bind first to the A sites and then to the B sites. When a Co(II) ion enters the B site, 3.9 Å from Co(II) in the A site, the second Co(II) ion causes a dramatic change in the magnetic environment of the A site Co(II), as shown by additional shifts in the proton signals originally paramagnetically shifted by Co(II) in the A sites alone.<sup>19</sup> In the case of Cu(II), a highly specific ESR spectrum with nitrogen hyperfine structure from three magnetically equivalent nitrogen atoms as ligands is observed on the binding of the first 2 equiv of Cu(II) to the apoalkaline phosphatase dimer.<sup>16</sup> This ESR spectrum has been assigned to Cu(II) in the A sites.<sup>16</sup> Detailed studies of alkaline phosphatase have focused on the highly active Zn(II) and Co(II) derivatives and on the Cd(II) derivative, which turns over 10<sup>2</sup>-10<sup>3</sup> times more slowly than the active metallophosphatases.<sup>4,22</sup> The Cd(II) enzyme has been characterized by <sup>113</sup>Cd NMR spectroscopy<sup>22</sup> and by X-ray crystallography.<sup>23,24</sup>

- (1) (a) University of Florence. (b) University of Bologna. (c) IBM T. J. Watson Center. (d) Yale University School of Medicine.
- (2) AP = alkaline phosphatase. In the species Cu<sub>2</sub>Mg<sub>2</sub>AP and Cu<sub>2</sub>Cu<sub>2</sub>AP, the first metal symbol and subscript refer to the metal ion species and number of metal ions in the A sites, while the second metal ion symbol and subscript refer to the metal ion species and number of metal ions in the B sites. E, as in Cu<sub>2</sub>E<sub>2</sub>AP, is the symbol for an "empty" site, i.e. no metal ion bound. E-P = the phosphorylated enzyme formed by the phosphorylation of Ser-102. E-P = the phosphoenzyme complex formed by the coordination of phosphate to the A-site metal ion, sometimes referred to as the "noncovalent" phosphate complex with alkaline phosphatase.
- (3) Bradshaw, R. A.; Cancedda, F.; Ericsson, L. H.; Newman, P. A.; Piccoli, S. P.; Schlesinger, M. J.; Sriefer, K.; Walsh, K. A. *Proc. Natl. Acad. Sci. U.S.A.* **1981**, *78*, 3473.
- (4) Coleman, J. E.; Gettins, P. *Adv. Enzymol. Relat. Areas Mol. Biol.* **1983**, *55*, 381.
- (5) Coleman, J. E.; Gettins, P. In *Zinc Enzymes*; Bertini, I., Luchinat, C., Maret, W., Zeepezauer, M., Eds.; Birkhauser: Boston, MA, 1986; Chapter 6.
- (6) Rothman, J.; Byrne, R. *J. Mol. Biol.* **1963**, *6*, 330.
- (7) Plocke, D. J.; Leveintal, C.; Vallee, B. L. *Biochemistry* **1962**, *1*, 373.
- (8) Plocke, D. J.; Vallee, B. L. *Biochemistry* **1962**, *1*, 1039.
- (9) Otvos, J. D.; Armitage, I. M. *Biochemistry* **1980**, *19*, 4021.
- (10) Anderson, R. A.; Bosron, W. F.; Kennedy, F. S.; Vallee, B. L. *Proc. Natl. Acad. Sci. U.S.A.* **1975**, *72*, 2989.
- (11) Bosron, W. F.; Falk, M. C.; Kennedy, F. S.; Vallee, B. L. *Biochemistry* **1977**, *16*, 610.
- (12) Bosron, W. F.; Kennedy, F. S.; Vallee, B. L. *Biochemistry* **1975**, *14*, 2275.
- (13) Wyckoff, H. W.; Handschumacher, M. D.; Murthy, K. H. M.; Sowadski, J. M. *Adv. Enzymol. Relat. Areas Mol. Biol.* **1983**, *55*, 453.
- (14) Sowadski, J. M.; Handschumacher, M. D.; Murthy, K. H. M.; Foster, B. A.; Wyckoff, W. *J. Mol. Biol.* **1985**, *186*, 417.

- (15) Csopak, H.; Falk, K. E. *FEBS Lett.* **1970**, *7*, 147.
- (16) Taylor, J. S.; Coleman, J. E. *Proc. Natl. Acad. Sci. U.S.A.* **1972**, *69*, 859.
- (17) Csopak, H.; Falk, K. E. *Biochem. Biophys. Acta* **1974**, *359*, 22.
- (18) Bertini, I.; Luchinat, C.; Scozzafava, A.; Maldotti, A.; Traverso, O. *Inorg. Chim. Acta* **1983**, *78*, 19.
- (19) Banci, L.; Bertini, I.; Luchinat, C.; Viezzoli, M. S.; Wang, Y. *J. Inorg. Biochem.* **1987**, *30*, 77.
- (20) Applebury, M. L.; Coleman, J. E. *J. Biol. Chem.* **1969**, *244*, 709.
- (21) Lazdunski, C.; Chappellet, D.; Peticlerc, C.; Leterrier, F.; Douzou, P.; Lazdunski, M. *Eur. J. Biochem.* **1970**, *17*, 239.
- (22) Gettins, P.; Coleman, J. E. *J. Biol. Chem.* **1983**, *58*, 396.
- (23) Wyckoff, H. W. In *Phosphate Metabolism and Cellular Regulation in Microorganisms*; Toriani-Gorini, A., Rothman, F. C., Silver, S., Wright, A., Yagil, E., Eds.; American Society for Microbiology: Washington, DC, 1987; p 120.

While the catalytic activity of the Cd(II) enzyme is too low to measure by the standard assays involving phosphate ester hydrolysis because of the unavoidable low levels of Zn(II) contamination, it is possible to follow phosphate turnover catalyzed by the Cd(II) enzyme with  $^{31}\text{P}$  NMR spectroscopy and show that all steps of the catalytic reaction occur with the Cd(II) enzymes.<sup>4,22-25</sup> Understanding the specific properties of several different transition- and IIB-metal ions bound at the multimetal active center of alkaline phosphatase may help to reveal the coordination chemistry required for catalysis. In the case of paramagnetic metal ions it is possible to monitor the magnetic interactions of the metal ion in the A site with the metal ion in the B site. It has been shown for example that in  $\text{Cu}_2\text{CO}_2\text{AP}^{2-}$  the electronic relaxation times of Cu(II) are reduced through magnetic interaction with Co(II).<sup>19</sup> The present paper presents a detailed study of  $\text{Cu}_2\text{Cu}_2\text{AP}$  and the interactions between  $\text{Cu}_A$  and  $\text{Cu}_B$  as measured by ESR spectroscopy, magnetic susceptibility, and nuclear magnetic resonance dispersion (NMRD).<sup>26-28</sup> A separate paper<sup>29</sup> presents a corresponding study of the manganese(II) alkaline phosphatase.

### Materials and Methods

Alkaline phosphatase from *E. coli* was isolated and purified as reported previously.<sup>25</sup> The apoprotein was prepared by dialysis against 2 M  $(\text{NH}_4)_2\text{SO}_4$ .<sup>22</sup> The activity of the apoenzyme was always <5% of that shown by the native protein. Protein concentrations were determined spectrophotometrically at 280 nm by using  $\epsilon_{280} = 6.768 \times 10^4 \text{ M}^{-1} \text{ cm}^{-1}$  and a molecular weight for the dimer of 94 000.<sup>3</sup> Unbuffered, salt-free apoenzyme solutions were used for the studies at pH 6, while 0.01 M Tris-HCl was used in the enzyme samples prepared at pH 8. Apoenzyme samples at various concentrations were obtained by stepwise dilutions of stock apoenzyme solutions concentrated to approximately 1 mM in a metal-free Amicon ultrafiltration device. Copper(II) was added stepwise as copper sulfate. X-Band ESR spectra at 298 or 77 K were run on a Bruker ER 200 spectrometer calibrated by using diphenylpicrylhydrazyl ( $g = 2.0037$ ). Water proton longitudinal relaxation measurements (NMRD) were performed at 298 K by using a field-cycling relaxometer described elsewhere,<sup>27,28</sup> in the proton Larmor frequency range 0.01–40 MHz. Sample volumes were 0.5–0.8 mL. Room-temperature susceptibility measurements were performed with the Evans method at 300 MHz using NaDSS (sodium 4,4-dimethyl-4-silapentane-1-sulfonate) as an inert standard and acetone as a secondary standard. The accuracy of the measurements is estimated to be  $\pm 0.1$  Hz over the total bulk susceptibility shifts of 5–10 Hz.  $^{31}\text{P}$  NMR spectra were recorded at 298 K on a Bruker 200 MSL instrument operating at 80.98-MHz frequency, equipped with a broad-band tunable probe. Samples were of 1.8-cm<sup>3</sup> volume and were contained in 10-mm tubes fitted with vortex plugs and a coaxial capillary containing  $\text{D}_2\text{O}$  for the field frequency lock. Broad-band proton decoupling was not employed. Chemical shifts are reported relative to 1% phosphoric acid solution.

### Results

**NMRD of Apoalkaline Phosphatase.** The apoprotein causes a large water  $^1\text{H}$   $T_1^{-1}$  enhancement owing to its large  $\tau_r$  value ( $MW = 94\,000$ ). The magnetic field dependence of the  $^1\text{H}$   $T_1^{-1}$  at various apoprotein concentrations is shown in Figure 1. The dispersions have been fit to an equation of the type<sup>27,28</sup>

$$T_{1(\text{dia})}^{-1} = T_{1(\text{water})}^{-1} + D + A \operatorname{Re} \left( \frac{1}{1 + (i\nu/\nu_c)^{\beta/2}} \right) \quad (1)$$

which has been found appropriate for relaxation enhancements caused by diamagnetic macromolecular solutes.<sup>26</sup>  $T_{1(\text{water})}^{-1}$  is the contribution of the solvent, taken equal to  $0.33 \text{ s}^{-1}$ ; Re means “the

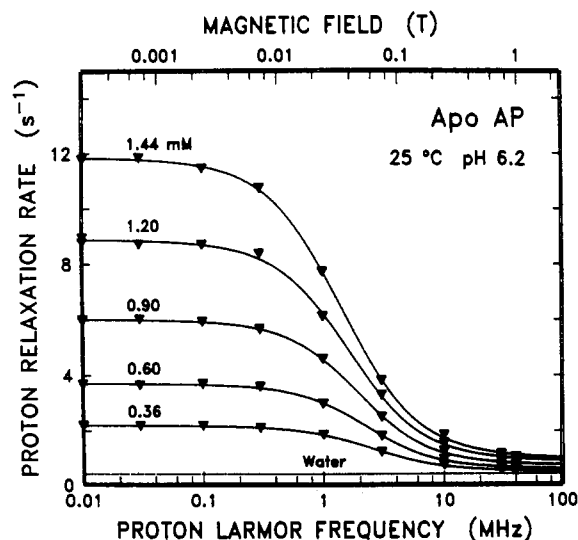


**Figure 1.** (▼) Observed  $T_1^{-1}$  NMRD profiles for five concentrations (0.36, 0.60, 0.90, 1.20, and 1.44 mM dimer) of *E. coli* apoalkaline phosphatase, at 298 K. The samples were in water, at pH 6. The background contribution of protein-free buffer (water) is also indicated. The smooth curves through the data points result from a least-squares fit of the data to eq 1.<sup>28</sup> The derived values for the four parameters of the fit for these and other sample concentrations are given in Table I. The variation of the field at which the curves inflect is concentration dependent because of increasing hydrodynamic interactions of the protein molecules with increasing protein concentration, a point previously considered in some detail.<sup>27</sup>

**Table I.** Best-Fitting Parameters<sup>a</sup> for the  $^1\text{H}$  NMRD Profiles of Apoalkaline Phosphatase at Different Concentrations

concn, mM	$A, \text{ s}^{-1}$	$\beta$	$\nu_c^b$ , MHz	$D, \text{ s}^{-1}$	$\tau_r^c, \mu\text{s}$
1.44	10.938	1.6986	1.4358	0.933 93	0.063 999
1.31	9.2881	1.7217	1.5727	0.895 06	0.058 427
1.20	8.0419	1.7238	1.6438	0.852 03	0.055 899
1.03	6.4145	1.7346	1.8178	0.749 47	0.050 548
0.90	5.2989	1.7524	1.9684	0.703 09	0.046 681
0.72	3.9314	1.7821	2.0315	0.632 92	0.045 231
0.60	3.1279	1.7699	2.3178	0.571 60	0.039 644
0.45	2.2289	1.7607	2.5048	0.509 64	0.036 685
0.36	1.7151	1.7432	2.5828	0.481 89	0.035 577

<sup>a</sup> The best fitting was performed by using eq 1 (see text). <sup>b</sup>  $\nu_c = 1/(2\pi(3^{1/2}\tau_r))$ . <sup>c</sup>  $\tau_r = 4\pi r^2\eta/(3\kappa T)$ .

real part of";  $D$  and  $A$  are the amplitudes of constant and dispersive contributions to the NMRD profile;  $\nu$  is the magnetic field in units of the Larmor frequency, and  $\nu_c = 1/(2\pi(3^{1/2}\tau_r))$ ; and  $\beta$  is a parameter that determines the slope of the profile at its inflection point.  $\tau_r$  is the rotational correlation time as defined in Table I. The values of the parameters giving the best fit are found in Table I. The effective  $\tau_r$  increases by a factor of 2 on increasing the protein concentration from 0.36 to 1.44 mM, whereas the exponent is constant within 2%. The data can be accounted for by a simple theory for microviscosity of solutions of macromolecular solutes.<sup>27,28</sup> While there is not a significant increase in the viscosity of the bulk solution over this range of protein concentration, the protein solution does not remain infinitely dilute. At high concentration the free rotation is hindered by the “boundary” of surrounding macromolecules, which cause an increase in effective  $\tau_r$  (Table I). The water proton NMRD of apoalkaline phosphatase is a particularly nice example of this function for a protein versus concentration, and the profile allows us to predict the relaxivity of the apoprotein at every intermediate concentration by interpolating between known values.

**Room-Temperature Optical Absorption and ESR Spectra of Cu(II) Alkaline Phosphatase.** Aside from early reports on the lack of activity of the copper enzyme,<sup>21,25</sup> no detailed descriptions of its properties have appeared except for an ESR study at liquid-nitrogen temperature, pH 8, showing that both Cu(II) ions

- (24) Coleman, J. E. In *Phosphate Metabolism and Cellular Regulation in Microorganisms*; Toriani-Gorini, A., Rothman, F. G., Silver, S., Wright, A., Yagil, E., Eds.; American Society for Microbiology: Washington, DC, 1987; p 127.
- (25) Applebury, M. L.; Johnson, B. P.; Coleman, J. E. *J. Biol. Chem.* **1970**, *245*, 4968.
- (26) Bertini, I.; Luchinat, C. *NMR of Paramagnetic Molecules in Biological Systems*; Benjamin-Cummings: Boston, MA, 1986.
- (27) Koenig, S. H. In *Water in Polymers*; Rowland, S. P., Ed.; ACS Symposium Series 127; American Chemical Society: Washington, DC, 1980; p 157.
- (28) Hallenga, K.; Koenig, S. H. *Biochemistry* **1976**, *15*, 4255.
- (29) Schulz, C.; Bertini, I.; Viezzoli, M.-S.; Brown, R. D.; Koenig, S. H.; Coleman, J. E. *Inorg. Chem.*, in press.

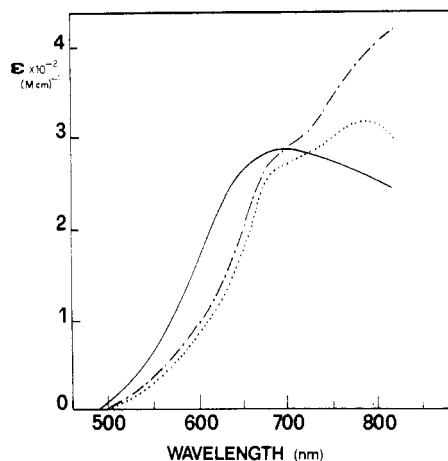


**Figure 2.** Visible absorption spectra of Cu<sub>2</sub>E<sub>2</sub>AP (—) and the same sample plus 2 equiv of inorganic phosphate (···). The latter spectrum was taken after 12 h to allow the spectral changes to be completed. An additional equivalent of Cu(II) was then added (-·-). Conditions: 0.01 M Tris-HCl, pH 8, 298 K, 1 mM enzyme.

of Cu<sub>2</sub>E<sub>2</sub>AP<sup>2</sup> occupy identical sites in the dimer, sites which were originally occupied by Zn(II).<sup>16</sup> The lowest field copper hyperfine line in the  $g_{\parallel}$  region of this ESR spectrum showed a seven-line nitrogen ligand hyperfine pattern, indicating that each Cu(II) ion is coordinated to three magnetically equivalent nitrogen atoms.<sup>16</sup> This conclusion is compatible with the later crystal structure of the Zn(II) enzyme, which shows three His residues (331, 372, and 412) and probably two solvent molecules ligated to the A-site Zn(II).<sup>14</sup>

Before descriptions of the NMRD profiles of the copper derivatives of alkaline phosphatase and their phosphate complexes are given, the spectroscopic properties of the various Cu(II) derivatives and their phosphate complexes with different copper/protein ratios are presented. Both the optical and the ESR spectra are recorded at room temperature under the same conditions that the NMRD profile was obtained. The Cu<sub>2</sub>E<sub>2</sub>AP at pH 8 has a broad absorption envelope,  $\epsilon_{690} = 290 \text{ M}^{-1} \text{ cm}^{-1}$  or  $145 \text{ M}^{-1} \text{ cm}^{-1}/\text{Cu(II)}$  ion (Figure 2). When 1 or 2 equiv of inorganic phosphate is added to the Cu<sub>2</sub>E<sub>2</sub>AP solution, there is a red shift in the d-d absorption maximum from 690 to 790 nm ( $\epsilon = 312 \text{ M}^{-1} \text{ cm}^{-1}$  or  $156 \text{ M}^{-1} \text{ cm}^{-1}/\text{Cu(II)}$  ion) (Figure 2). A prominent shoulder remains, however, at 690 nm in the absorption spectrum of the phosphate complex. The phosphate-induced change in the d-d transitions of Cu(II) is time-dependent, and the complete change requires several hours. Addition of a third equivalent of Cu(II) results in an additional increase in optical absorption near 800 nm (Figure 2), suggesting that Cu(II) in the B sites absorbs at considerably lower energy. A fourth equivalent of Cu(II) was not added, since in contrast to pH 6 (see below) part of the fourth equivalent of Cu(II) added at pH 8 forms a complex with Tris buffer (absorbing at 600 nm). Tris, or any other buffer used to solubilize Cu(II), is a better ligand at pH 8 than at pH 6.

Cu<sub>2</sub>E<sub>2</sub>AP at pH 8 has a homogeneous ESR signal at room temperature with  $g_{\parallel} = 2.32$ ,  $g_{\perp} = 2.09$ , and  $A_{\parallel} = 164 \times 10^{-4} \text{ cm}^{-1}$  (Figure 3A), values similar to those reported previously at liquid-nitrogen temperature.<sup>16</sup> Mg(II) when present at 10 mM concentration is known to occupy the B sites, 3.9 Å from the A sites.<sup>24</sup> While the room-temperature ESR spectrum of the Cu<sub>2</sub>Mg<sub>2</sub>AP is generally similar to that of the same enzyme without Mg(II), there are significant changes in the spectral parameters, with  $g_{\parallel} = 2.34$ ,  $g_{\perp} = 2.09$ , and  $A_{\parallel} = 151 \times 10^{-4} \text{ cm}^{-1}$  (Figure 3B). These changes in the ESR parameters show that the precise chemical environment of Cu(II) in the A sites is changed when a metal ion occupies the adjacent B site; the smaller  $A_{\parallel}$  may involve a change from a tetragonal complex to one with some tetrahedral distortion as Mg(II) occupies the B site.

Addition of 2 equiv of inorganic phosphate to the Cu<sub>2</sub>Mg<sub>2</sub>AP induces a decrease in the intensity of the room-temperature ESR signal, which has lost 60% of its intensity by 3 h (Figure 3C). This

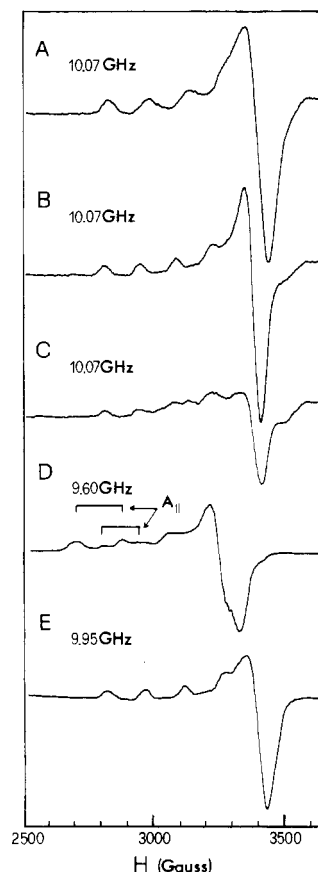


**Figure 3.** ESR spectra of Cu(II) alkaline phosphatase at room temperature (298 K; A–C, E) and liquid-nitrogen temperature (77 K; D): (A) Cu<sub>2</sub>E<sub>2</sub>AP, pH 8; (B) Cu<sub>2</sub>Mg<sub>2</sub>AP, pH 8; (C) sample B plus 2 equiv of inorganic phosphate, after 3-h incubation; (D) Cu<sub>2</sub>E<sub>2</sub>AP, pH 8, plus 2 equiv of inorganic phosphate at 77 K, after 24-h incubation at room temperature; (E) Cu<sub>2</sub>E<sub>2</sub>AP, pH 6.

fall in intensity can be interpreted as a migration of Cu(II) from the A site of one monomer (without bound phosphate) to the B site of the other monomer (with bound phosphate), which gives rise to antiferromagnetic coupling (see below). Such a phosphate-induced migration can also account for the changes in the d-d absorption spectrum (see Discussion). This same fall in the amplitude of the room-temperature ESR signal is observed when phosphate is added to Cu<sub>2</sub>E<sub>2</sub>AP, but it occurs more slowly than in the presence of Mg(II) in the B sites (see Discussion). An ESR spectrum of the noncovalent phosphoenzyme formed by Cu<sub>2</sub>E<sub>2</sub>AP can still be observed at liquid-nitrogen temperature (Figure 3D). This spectrum consists of two overlapping spectra of approximately equal intensity, one like the original spectrum ( $A_{\parallel} = 189 \times 10^{-4} \text{ cm}^{-1}$ ) and a new one with smaller  $A_{\parallel}$  value ( $A_{\parallel} = 149 \times 10^{-4} \text{ cm}^{-1}$ ). The ESR spectra obtained at pH 6 are similar to those obtained at pH 8, as shown by the spectrum of Cu<sub>2</sub>E<sub>2</sub>AP ( $g_{\parallel} = 2.31$ ,  $g_{\perp} = 2.07$ ,  $A_{\parallel} = 161 \times 10^{-4} \text{ cm}^{-1}$ ) in Figure 3E.

**Phosphate Binding by Cu(II) Alkaline Phosphatase As Detected by <sup>31</sup>P NMR Spectroscopy.** The binding of phosphate to alkaline phosphatase can be followed by <sup>31</sup>P NMR spectroscopy.<sup>4,22,24,30,31</sup> <sup>31</sup>P NMR spectra recorded during the titration of Cu<sub>2</sub>E<sub>2</sub>AP with inorganic phosphate are shown in Figure 4. One mole of P<sub>i</sub> added per mole of enzyme dimer at pH 8 results in a <sup>31</sup>P NMR signal broadened beyond detection (Figure 4B). This occurs as rapidly as a signal for free phosphate can be observed at millimolar concentrations, approximately 10 min. Hence, the changes over several hours in the optical and ESR spectra of the phosphate complex do not appear to reflect the slow binding of phosphate.

(30) Chlebowski, J. F.; Armitage, I. M.; Coleman, J. E. *J. Biol. Chem.* **1977**, *252*, 7053.

(31) Weiner, R. E.; Chlebowski, J. F.; Haffner, P. H.; Coleman, J. E. *J. Biol. Chem.* **1979**, *254*, 9739.

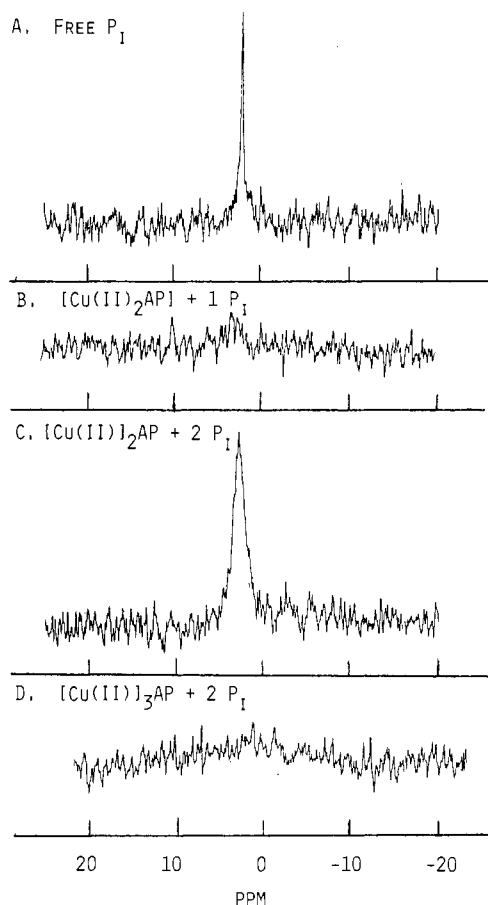


**Figure 4.**  $^{31}\text{P}$  NMR signals of inorganic phosphate in the presence of  $\text{Cu}_2\text{E}_2\text{AP}$  (1 mM), at 298 K: (A) 1 mM inorganic phosphate in 0.01 M Tris-HCl, pH 8; (B) 1 mM enzyme plus 1 equiv of inorganic phosphate in 0.01 M Tris-HCl, pH 8; (C) 1 mM enzyme plus 2 equiv of inorganic phosphate added to  $\text{Cu}_2\text{E}_2\text{AP}$  at zero time in 0.01 M Tris-HCl, pH 8; (D) sample C plus an additional equivalent of Cu(II).

In contrast, when a second equivalent of  $\text{P}_i$  is added to  $\text{Cu}_2\text{E}_2\text{AP}$ , a signal appears at the resonance position of free  $\text{P}_i$  (Figure 4C). From these data it is clear that  $\text{Cu}_2\text{E}_2\text{AP}$  binds phosphate in the same manner as documented for other  $\text{M}_2\text{E}_2\text{AP}$  derivatives:<sup>4</sup> only one phosphate ion is bound per dimer; i.e., phosphate is bound negatively cooperatively to the enzyme containing only two Cu(II) ions in the A sites. As in the case of  $\text{Co}_2\text{E}_2\text{AP}$  and  $\text{Mn}_2\text{E}_2\text{AP}$ , the  $^{31}\text{P}$  resonance of the bound phosphate is broadened beyond detection.<sup>30,31</sup> Earlier studies have also shown that if the adjacent B metal-binding sites are occupied, a second mole of phosphate is bound.<sup>4</sup> In the case of the zinc enzyme this second mole of phosphate is bound less tightly.<sup>4,22</sup> Addition of a third Cu(II) ion to  $\text{Cu}_2\text{E}_2\text{AP} + 2\text{P}_i$  broadens the  $^{31}\text{P}$  signal to approximately 30 ppm (Figure 4D). In contrast to the signal from the first mole of  $\text{P}_i$  added, the  $^{31}\text{P}$  signal is broad but still detectable, which suggests that there is now intermediate exchange between free and bound phosphates, since at least 0.5 equiv of free phosphate should still remain at a 3:1 Cu(II):protein ratio.

Since the addition of the third equivalent of Cu(II) induces binding of a significant fraction of the second phosphate dianion (Figure 4D), it is likely that the binding of the third Cu(II) is cooperative. While some of the AP molecules at the 3:1 Cu(II):protein ratio probably have the composition  $\text{Cu}_2\text{Cu}_1\text{AP}\cdot\text{P}_1$ , most are probably divided relatively equally between  $\text{Cu}_2\text{Cu}_2\text{AP}\cdot\text{P}_2$  and  $\text{Cu}_1\text{Cu}_1\text{AP}\cdot\text{P}_1$ . We cannot detect significant phosphorylation of Ser-102 by  $^{32}\text{P}$ -phosphate labeling;<sup>25</sup> thus, the phosphate complex of the Cu(II) enzyme must be the metal-bound phosphate, E·P. In both the Cd(II) and Zn(II) enzymes E·P has been shown unequivocally to involve coordination of the phosphate to the A-site metal ion.<sup>4,24</sup>

**Nuclear Magnetic Resonance Dispersion (NMRD) of Copper(II) Alkaline Phosphatase.** Since  $\text{Cu}_2\text{E}_2\text{AP}$  is a spectroscop-

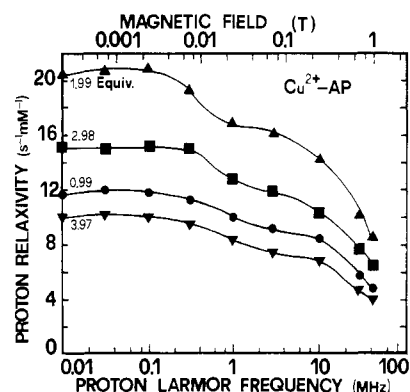


**Figure 5.**  $^1\text{H}$  NMRD profile for the Cu(II)-AP system at 298 K, pH 6, for four different Cu(II):protein ratios: 0.99 (●), 1.99 (▲), 2.98 (■), and 3.97 (▼) equiv of Cu(II)/equiv of dimer of alkaline phosphatase.

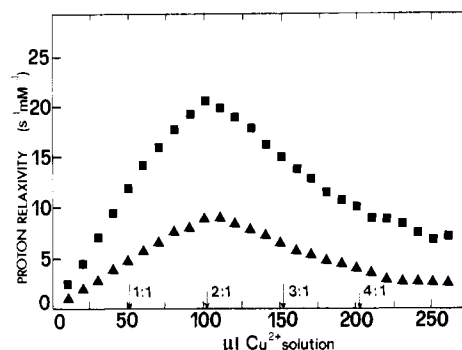


**Figure 6.** Relaxivity at 0.01 (■) and 40 MHz (▲) for titration of a 6.05 mM solution of Cu(II) ions ( $\text{CuSO}_4$ ) into 0.61 mM apoalkaline phosphatase at 298 K, pH 6. The points corresponding to 1:1, 2:1, 3:1, and 4:1 Cu(II):protein ratios are indicated on the abscissa.

ically well-defined species (Figures 2 and 3), the complete NMRD was first determined for the species resulting from the titration of apoalkaline phosphatase with 0.5–2 equiv of Cu(II) at pH 6. Examples of the complete  $T_1^{-1}$  NMRD profiles at 1.02 and 2.04 equiv of Cu(II)/equiv of enzyme dimer are shown in Figure 5. In this case, water proton longitudinal relaxation rates are the sum of three factors:<sup>26</sup>

$$T_1^{-1} = T_{1(\text{water})}^{-1} + T_{1(\text{dia})}^{-1} + T_{1\text{p}}^{-1} \quad (2)$$

where  $T_{1(\text{water})}^{-1}$ ,  $T_{1(\text{dia})}^{-1}$ , and  $T_{1\text{p}}^{-1}$  are the water, the apoenzyme, and the paramagnetic contributions, respectively, to the relaxation rate of the solvent water protons. The latter is related to  $T_{1\text{M}}^{-1}$ , the effect of the paramagnetic center on the exchangeable protons, through the equation

$$T_{1\text{p}}^{-1} = f(\tau_m + T_{1\text{M}})^{-1} \quad (3)$$

where  $f$  is the molar fraction of solvent nuclei interacting with the paramagnetic center and  $\tau_m$  is the lifetime of the metal ion–water adduct. This equation has been verified by performing measurements at various protein concentrations. In the case of  $\tau_m \ll T_{1\text{M}}$ , the relation  $T_{1\text{p}}^{-1} = fT_{1\text{M}}^{-1}$  holds.<sup>19</sup>

The enhancement of the relaxation of bulk water shown by the addition of the first 2 equiv of Cu(II) to apoalkaline phosphatase at pH 6 is substantial, rising to  $\approx 17$  ( $\text{mM s}^{-1}$ ) at a frequency of 0.01 MHz. Nearly identical results are observed at pH 8 (see below). In contrast, when a third equivalent of Cu(II) is added, there is a rapid fall in the paramagnetic contribution to the relaxivity of the protein (Figure 5); the relaxivity has fallen from 16 to 10 ( $\text{mM s}^{-1}$ ) at a frequency of 0.01 MHz. Addition of 4 equiv of Cu(II)/equiv of enzyme dimer leads to a further decrease in the paramagnetic contribution to the relaxivity, to  $\approx 7.5$  ( $\text{mM s}^{-1}$ ) at a 4:1 ratio. The NMRD profile is complicated by the appearance of small amounts of free Cu(II), but the contribution of this free Cu(II) to the relaxivity is low because of its short  $\tau_r$ . This will be discussed further below.

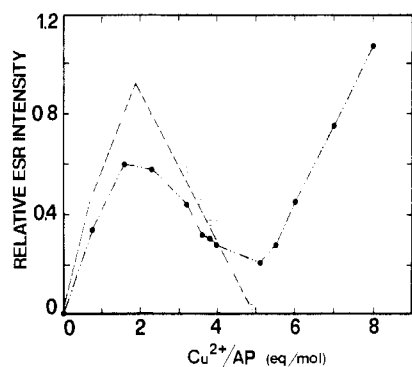


**Figure 7.** (●) Integrated intensity of the room-temperature (298 K) X-band ESR spectra of Cu(II) alkaline phosphatase in the  $g_{\perp}$  region as a function of the Cu(II):protein ratio. The peak in this function near the 2:1 ratio corresponds to the peak observed in Figure 6. The increase in signal intensity after 4–5 equiv of Cu(II) ions is added to the protein represents free Cu(II). (○) Intensity of the  $m_l = +1/2$   $g_{\parallel}$  Cu hyperfine line, which represents only the signal from enzyme-bound Cu(II).

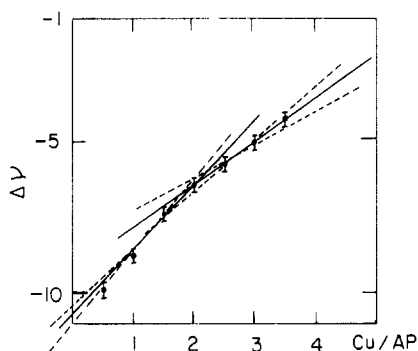


**Figure 8.** Differences in the chemical shift of the  $^1\text{H}$  NMR signal of DSS in water and in an aqueous solution of apoalkaline phosphatase as a function of increasing Cu(II):protein ratios in the enzyme solution. Conditions: 1.2 mM apoalkaline phosphatase in water at 298 K, pH 6. Cu(II) was added as a water solution of  $\text{CuSO}_4$ .

The decrease in relaxivity generated by the addition of 2–4 equiv of Cu(II)/equiv of enzyme dimer at pH 6 is graphically illustrated by plotting relaxivity at fields of 0.01 and 40 MHz as a function of Cu(II) concentration with the stoichiometric Cu(II):enzyme dimer ratios indicated on the abscissa (Figure 6). The increase in  $T_{1M}^{-1}$  is associated with Cu(II) populating a pair of binding sites in AP, the A sites, which must be accompanied by the simultaneous binding of water to the paramagnetic center.

**Antiferromagnetic Coupling between  $\text{Cu(II)}_A$  and  $\text{Cu(II)}_B$  in Alkaline Phosphatase.** The decrease in the relaxivity of the  $\text{Cu}_2\text{E}_2\text{AP}$  induced by the addition of a third equivalent of Cu(II) at pH 6 (Figures 5 and 6) correlates with a loss in the integrated intensity of the Cu(II) ESR spectrum of the enzyme at room temperature (298 K). The integrated intensity of the  $g_{\perp}$  region of the Cu(II) ESR signal during the sequential additions of 1–8 equiv of Cu(II)/equiv of alkaline phosphatase dimer is plotted in Figure 7. The intensity of the Cu(II) ESR signal increases up to the addition of 2 equiv of Cu(II) but then falls by 75% upon the addition of 3 and 4 equiv. Increases in the intensity of the  $g_{\perp}$  signal at higher ratios of Cu(II) are due to the appearance of free Cu(II) in solution at pH 6.

At the higher Cu(II):enzyme ratios, the  $g_{\perp}$  signal is not an accurate reflection of the change in the amplitude of the signal from the enzyme alone. Hence, we have also plotted in Figure 7 the intensity of the  $m_l = +1/2$  line in the  $g_{\parallel}$  region, which reflects only the enzyme signal. The intensity of the  $m_l = +1/2$  line has almost vanished at a Cu(II):enzyme ratio of 4:1. Thus, as the B sites, 3.9 Å from the Cu(II) ions in the A sites, are filled, there is almost a complete disappearance of the ESR signal (Figure 7). Both the ESR and the NMRD suggest the possibility that magnetic coupling is present between the A- and B-site Cu(II) ions in  $\text{Cu}_2\text{Cu}_2\text{AP}$ . However, no evidence was found of a  $\Delta m_s$ ,

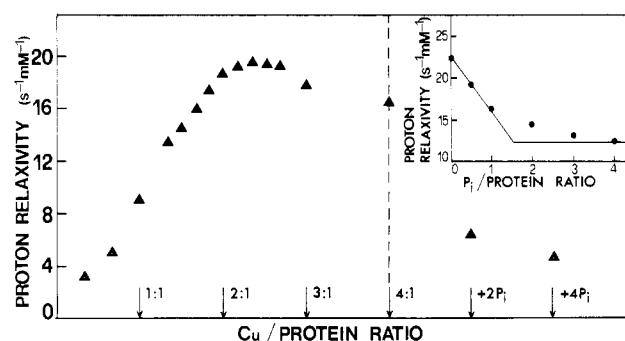
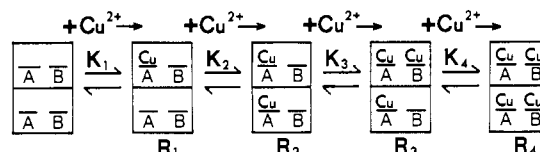


**Figure 9.** Relaxivity at 0.01 MHz during the titration of a solution of apoalkaline phosphatase with a 0.61 mM solution of Cu(II) ions ( $\text{CuSO}_4$ ) at 298 K. The enzyme was in 0.01 M Tris-HCl, pH 8. Cu(II):enzyme dimer ratios range from 0 to 4:1. Following the last addition of Cu(II) to give a ratio of 4:1, 2 and then 4 equiv of inorganic phosphate/equiv of enzyme dimer was added, and the relaxivity was measured, as indicated by the arrows. Inset: Relaxivity induced by  $\text{Cu}_2\text{E}_2\text{AP}$  as a function of added inorganic phosphate (●).

#### Scheme I



=  $\pm 2$  transition in the ESR spectrum at either room temperature or liquid-nitrogen temperature.

In order to further explore the nature of the magnetic interaction, room-temperature magnetic susceptibility measurements were performed with the Evans method at 300 MHz on an apoenzyme sample reacted with increasing amounts of Cu(II) (Figure 8). The molar susceptibility of the sample increases linearly from 0 to a 2:1 Cu(II):protein ratio and then increases with a smaller slope from ratios of 2:1 to 4:1. The change in slope from the first 2 to the second 2 equiv of Cu(II) added is outside the most extreme range for the experimental error, as shown by the dashed lines in Figure 8, and is further evidence of a magnetic coupling between Cu(II) ions in the A and B sites. If it is assumed that the magnetic susceptibility for the A and B sites in the isolated form is the same, from the change in slope a  $J$  of approximately 120  $\text{cm}^{-1}$  can be calculated as characterizing the antiferromagnetic coupling between the Cu(II) ions in the A and B sites of alkaline phosphatase.

**NMRD of Copper Alkaline Phosphatase at pH 8: Effect of Phosphate.** Relaxivity of the enzyme at pH 8 as a function of Cu(II):protein stoichiometry is shown in Figure 9. As observed at pH 6, the relaxivity rises steeply to 18 ( $\text{mM s}^{-1}$ ) at a 2:1 Cu(II):enzyme ratio as Cu(II) progressively occupies the A sites. There is a decline in relaxivity with the addition of the third equivalent of Cu(II). However, unlike the case at pH 6, when the fourth equivalent of Cu(II) is added, the relaxivity does not continue to fall in the absence of phosphate. If 2 equiv of phosphate is added, the relaxivity falls to a value less than 20% of that shown by  $\text{Cu}_2\text{E}_2\text{AP}$ . Addition of 4 equiv of  $\text{P}_i$  to the sample containing the 4:1 Cu(II):enzyme ratio causes the relaxivity to fall to approximately 7 ( $\text{mM s}^{-1}$ ) (Figure 9). A reasonable explanation is that there is more "free" or Tris-bound Cu(II) at pH 8, and the phosphate ligand drives the final equivalent of Cu(II) into the B site (see Discussion). A related effect of phosphate binding on the relaxivity of  $\text{Cu}_2\text{E}_2\text{AP}$  is observed when this species is titrated with phosphate (inset to Figure 9). The best explanation for the fall in relaxivity as phosphate is bound to  $\text{Cu}_2\text{E}_2\text{AP}$  is that phosphate binding to one A site causes migration of Cu(II) from the A site of the phosphate-free monomer to the B site of the phospho monomer, consistent with the loss of amplitude in the ESR spectra (see Discussion).

#### Discussion

**Equilibria between Cu(II) and Apoalkaline Phosphatase: Data Analysis.** On the assumption that the binding sequence of Scheme

I holds, with  $K_1 > K_2 > K_3 > K_4$ , a satisfactory fitting of the 0.01-MHz data in Figures 5 and 6 can be obtained with the following parameters:  $K_1 = 10^{10}$ ,  $K_2 = 10^7$ ,  $K_3 = 3 \times 10^4$ ,  $K_4 = 2.5 \times 10^3 \text{ M}^{-1}$ ;  $R_1 = 12$ ,  $R_2 = 21$ ,  $R_3 = 12$ ,  $R_4 = 1$ ,  $R_5 = 2 \text{ (mM s)}^{-1}$ .  $R_1$  to  $R_4$  are the relaxivities at 0.01 MHz of species 1 to 4, and  $R_5$  is the relaxivity of free Cu(II) at pH 6.

**Fitting of the Dispersion Data.** The dispersion curve for  $\text{Cu}_2\text{E}_2\text{AP}$  has been taken as representative of Cu(II) in the A site (Figure 5). The curve has been analyzed according to the following equation, assuming that there is only a dipolar contribution to the  $T_{1M}^{-1}$  enhancement:<sup>22</sup>

$$T_{1M}^{-1} = K \cdot G \cdot f(\tau_c, \nu, \theta) \quad (4)$$

$G$  is a geometrical factor,  $G = \sum_i (n_i / r_i^6)$ ;  $n_i$  is the number of protons at a distance  $r_i$  from the metal ion;  $\sum_i n_i$  is the total number of exchangeable protons interacting with the metal ion;  $f(\tau_c, \nu, \theta)$  describes the appropriate dependence of  $T_{1M}^{-1}$  on  $\tau_c$ , on the magnetic field, and on the angle  $\theta$  between the proton-metal vector and the  $z$  molecular axis.  $K$  is a constant containing some nuclear and electronic parameters. The fitting provides a  $G$  value of  $3.5 \times 10^{-15} \text{ pm}^{-6}$ , which corresponds to a single water molecule coordinated to A-site Cu(II) with a Cu-O distance of approximately 2 Å. The value of  $\tau_c$  is  $4 \times 10^{-9} \text{ s}$ , which is a typical value for electronic relaxation time for copper in tetragonal Cu(II) complexes.<sup>26,33</sup>

#### Structure of the Active Center of Cu(II) Alkaline Phosphatase.

A through-space dipolar interaction between the two A- and B-site Cu(II) ions approximately 4 Å apart could be enough to account for the loss of the Cu(II) ESR signal on the transition from  $\text{Cu}_2\text{E}_2\text{AP}$  to  $\text{Cu}_2\text{Cu}_2\text{AP}$  (Figure 7). The multiplicity of energy levels available for ESR transitions is increased by the spin-spin interaction, which can spread out the spin density, resulting in the loss of amplitude.

As Cu(II) occupies the B sites, there is a dramatic fall in the relaxivity (Figure 6). Any  $|J| \gg \hbar \tau_s^{-1}$  for the metal ions in a magnetically coupled homodinuclear species is expected to reduce the relaxation enhancement caused by each metal ion by half.<sup>34,35</sup> Hence, a relatively small  $J$  coupling could reduce the relaxivity produced by the A-site Cu(II) up to 50%. When a third Cu(II) ion is bound by the enzyme, however, the relaxivity becomes equal to that of  $\text{Cu}_2\text{E}_2\text{AP}$  (Figure 6). This finding and the previous analysis both suggest that  $\text{Cu}_2\text{Cu}_2\text{AP}$  has only residual relaxivity, much less than 50% of that of  $\text{Cu}_2\text{E}_2\text{AP}$ . This very large fall in relaxivity raises the following significant points concerning structure at the active center in the presence of Cu(II) ions.

Is it possible that the binding of the B-site Cu(II) displaces the bound water from the A-site Cu(II) ion? The Cu(II) ESR signal from the A site is axially symmetric (Figure 3), and under proper conditions at liquid-nitrogen temperature, seven nitrogen hyperfine lines are observed,<sup>16,17</sup> suggesting that Cu(II) in the A site is square-planar with the three nitrogen donors of His-412, -372, and -331 lying nearly in the plane. The exchangeable water ligand may also be in the plane as the dispersion fitting suggests with a bond length of 2 Å. While the B site is 3.9 Å from the A site, the crystal structures of the Zn(II) and Cd(II) enzymes show that the B site does not share any ligands with the A site.<sup>14</sup> It is possible that in the case of  $\text{Cu}_2\text{Cu}_2\text{AP}$ , i.e. when both A and B sites are occupied, the water becomes a bridging ligand, perhaps as  $\text{Cu}_A\text{-OH-Cu}_B$ . This structure with one bridging hydroxyl was found in some dinuclear copper(II) complexes in which a strong antiferromagnetic coupling is operative.<sup>36</sup> In contrast, bridging formation has less tendency to form in the analogous Co(II) or

Mn(II) pair and magnetic susceptibility data do not suggest a bridging ligand for the Co(II)<sup>19</sup> or Mn(II)<sup>29</sup> derivatives of alkaline phosphatase or for the  $\text{Cu}_2\text{Co}_2\text{AP}$  mixed derivative.<sup>19</sup>

On the other hand, the hydroxyl of Ser-102 is located just off the axis connecting the A and B metal ions. It is also possible that Cu(II) in occupying the B site becomes bound to Ser-O, which could become a bridging ligand between Cu(II)<sub>A</sub> and Cu(II)<sub>B</sub>, displacing the water ligand of Cu(II)<sub>A</sub>. Either of the above structures would explain the relatively large value of  $J$ , approximately  $120 \text{ cm}^{-1}$ , estimated from the susceptibility measurement (Figure 8), a  $J$  value that requires a through-bond magnetic coupling for two Cu(II) ions. As a corollary to the above arguments, the very low relaxivity observed for  $\text{Cu}_2\text{Cu}_2\text{AP}$  suggests that if Cu(II) in the B site carries any coordinated water with it, such water cannot be in rapid exchange with bulk water.

Does phosphate binding to  $\text{Cu}_2\text{Cu}_2\text{AP}$  displace a bound water? In  $\text{Zn}_2\text{Zn}_2\text{AP}$  and  $\text{Cd}_2\text{Cd}_2\text{AP}$  the phosphate ligand is directly coordinated to the A-site metal ion.<sup>4,5,22,24</sup> One would ordinarily expect such a ligand to displace bound water. However, in the Zn(II) and Cd(II) enzymes the three His nitrogens are not planar,<sup>3,14,23</sup> and <sup>35</sup>Cl NMR spectroscopy combined with phosphate binding clearly shows the A site in these derivatives to be 5-coordinate with two coordination sites available for water,<sup>37</sup> a conclusion supported by the crystal structure.<sup>14</sup> It is thus possible that phosphate binds to the Cu(II) of the A site in a more or less axial position in a square-planar or tetragonally distorted Cu(II) complex, displacing a distant water that makes little contribution to the relaxivity. This would explain why the relaxivity of  $\text{Cu}_2\text{Cu}_2\text{AP}$  with bound phosphate (Figure 9) is not substantially different from that of  $\text{Cu}_2\text{Cu}_2\text{AP}$  alone (Figures 5 and 6).

What process causes the changes in relaxivity upon the addition of phosphate to  $\text{Cu}_2\text{E}_2\text{AP}$ ? As one or more phosphate ions are added to this species, the relaxivity falls and drifts downward with time (Figure 9). This might be interpreted as a simple displacement of exchangeable water, but the amplitude of the room-temperature ESR spectrum is lost in a manner that correlates with the time-dependent, phosphate-induced loss of relaxivity (Figure 3C). Inspection of all the spectral changes accompanying phosphate binding to  $\text{Cu}_2\text{E}_2\text{AP}$  suggests that Cu(II) migrates from the A site of the monomer with no bound phosphate to the B site of the monomer with bound phosphate to form the very stable  $\text{Cu}_A\text{Cu}_B\text{-P}_i$  complex on a single monomer. Collection of the <sup>31</sup>P NMR data shows that as soon as a signal can be observed for the  $\text{Cu}_2\text{E}_2\text{AP}$  samples (10 min), half the <sup>31</sup>P signal has disappeared if 2 equiv of  $\text{P}_i$  is present and all has disappeared if 1 equiv of  $\text{P}_i$  is present (Figure 4). This occurs before the ESR (Figure 3) or the relaxivity (Figure 9) of the samples has changed. Thus, phosphate binding induces metal ion migration.

The drop in the amplitude of the ESR signal must result from a spin-spin interaction, and the migration of one of the two Cu(II) ions in the enzyme appears to be the only mechanism of creating such a spin-spin interaction, i.e. similar to that which occurs between the A and B sites in  $\text{Cu}_2\text{Cu}_2\text{AP}$ . Over a similar time period a new d-d absorption envelope appears centered at 790 nm (Figure 2), and the unpaired electrons of approximately half the Cu(II) ions shift to a new environment with a larger  $g_{\perp}$  and a significantly smaller  $A_{\parallel}$  (Figure 3D), also with a similar time dependence. The 790-nm absorption maximum also appears in  $\text{Cu}_2\text{Cu}_2\text{AP}$  and is likely to arise from Cu(II) bound to the B sites (Figure 2).

A migration of a Cd(II) ion from the A site of an unphosphorylated monomer to the B site of a phosphorylated monomer has been well documented following phosphorylation of  $\text{Cd}_2\text{E}_2\text{AP}$ .<sup>22</sup> Only one monomer of the  $\text{Cd}_2\text{E}_2\text{AP}$  becomes phosphorylated, and this induces the slow migration of Cd(II) from the unphosphorylated monomer to form the highly stable  $\text{Cd}_A\text{Cd}_B$  phosphoseryl-102 complex at one active center.<sup>22,24</sup> <sup>31</sup>P NMR spectroscopy shows 1 mol of phosphate to bind per  $\text{Cd}_2\text{E}_2\text{AP}$  within the few minutes it takes to collect the <sup>31</sup>P signal. <sup>113</sup>Cd NMR spectroscopy shows Cd(II) to remain in the A sites until well after

(32) Bertini, I.; Briganti, F.; Luchinat, C.; Mancini, M.; Spina, G. *J. Magn. Reson.* **1985**, *63*, 41.

(33) Bertini, I.; Briganti, F.; Koenig, S. H.; Luchinat, C. *Biochemistry* **1985**, *24*, 6287.

(34) Owens, C.; Drago, R. S.; Bertini, I.; Luchinat, C.; Banci, L. *J. Am. Chem. Soc.* **1986**, *108*, 3298.

(35) Bertini, I.; Banci, L.; Brown, R. D.; Koenig, S. H.; Luchinat, C. *Inorg. Chem.* **1988**, *27*, 951.

(36) (a) Haddad, M. S.; Hendrickson, D. N. *Inorg. Chim. Acta* **1978**, *28*, L221. (b) Haddad, M. S.; Wilson, S. R.; Hodgson, D. J.; Hendrickson, D. N. *J. Am. Chem. Soc.* **1981**, *103*, 384.

(37) Gettins, P.; Coleman, J. E. *J. Biol. Chem.* **1984**, *259*, 11036.

the initial binding of phosphate. The slow migration of  $^{113}\text{Cd}(\text{II})$  to the opposite B site is then observed to be a slow process with a half-time of 17 h. Likewise, only one monomer of  $\text{Cu}_2\text{E}_2\text{AP}$  binds phosphate (Figure 4), and the same migration appears to best account for all the spectroscopic data.

The initial event that prevents the second A site from binding phosphate and restoring symmetry to the dimer, prior to the metal ion migration, must be a conformational change accompanying phosphorylation of one monomer and propagated across the monomer-monomer interface. Once this conformational change has occurred, the affinities of a particular species of metal ion for the unliganded A site relative to the affinity (of the same metal ion) for the B site adjacent to a phosphorylated A site must determine whether migration of the metal ion occurs. No evidence of phosphate-induced migration has been found in the case of the  $\text{Zn}_2\text{E}_2\text{AP}$ ,<sup>24</sup>  $\text{Co}_2\text{E}_2\text{AP}$ ,<sup>24</sup> or  $\text{Mn}_2\text{E}_2\text{AP}$ <sup>29</sup> enzymes, despite the fact that only one monomer becomes phosphorylated in these species as well. On the other hand, migration appears to be induced by phosphorylation in the case of  $\text{Cd}_2\text{E}_2\text{AP}$  or phosphate binding to A-site  $\text{Cu}(\text{II})$  in the case of  $\text{Cu}_2\text{E}_2\text{AP}$ .

Data obtained by several spectroscopic probes show that the A-site metal ion senses the presence of the B-site metal ion, despite the fact that the two sites in most cases do not appear to share a ligand. This same phenomenon can be observed in the  $\text{Cu}_A\text{Mg}_B$

mixed species, as shown by the change in the ESR signal of  $\text{Cu}_2\text{E}_2\text{AP}$  when  $\text{Mg}(\text{II})$  occupies the B site (Figure 3B). This binding of  $\text{Mg}(\text{II})$  to the B site may actually destabilize  $\text{Cu}_A$  by distorting the A site, since the phosphate-induced migration of one of the A-site  $\text{Cu}(\text{II})$  ions to the opposite B site occurs more rapidly in the presence of  $\text{Mg}(\text{II})$ . While not normally sharing a ligand, sites A and B do share a small section of polypeptide chain, since His-370 is ligated to the B-site metal, while His-372 is ligated to the A-site metal.<sup>14</sup> Thus, the two ligands are separated only by Ala-371 and a conformational change upon binding of metal ion to the B site could be propagated along this short region of the peptide chain.

It is possible that the square-planar nature of the  $\text{Cu}(\text{II})$  complex places the phosphate ligand in an unusual position relative to the hydroxyl of Ser-102 and thus prevents phosphorylation of the enzyme. In the case of the paramagnetic derivative of alkaline phosphatase formed with four  $\text{Mn}(\text{II})$  ions, there is no magnetic coupling between the A- and B-site metal ions<sup>29</sup> and the enzyme does phosphorylate Ser-102.<sup>25</sup>

**Acknowledgment.** This work was supported by NIH Grant DK09070-23 and NATO Collaborative Research Grant D.0021/88.

**Registry No.** AP, 9001-78-9;  $\text{PO}_4^{3-}$ , 14265-44-2; Cu, 7440-50-8.

Contribution from the Institute of Physical and Chemical Research, Wako-shi, Saitama 351-01, Japan

## Crystal Structure of a Silver Salt of the Antibiotic Lasalocid A: A Dimer Having an Exact 2-fold Symmetry

Il-Hwan Suh, Katsuyuki Aoki,\* and Hiroshi Yamazaki

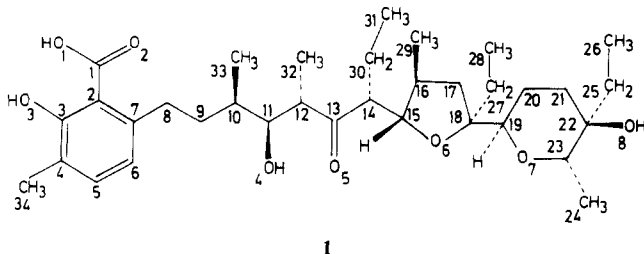
Received June 3, 1988

The crystal structure of a silver salt of the antibiotic lasalocid A, prepared from lasalocid A sodium salt and silver perchlorate in aqueous acetone, has been determined by X-ray analysis. The salt forms two types of "head-to-tail" dimers, which share a common crystallographic 2-fold rotation axis in the crystal lattice; both dimeric structures are, therefore, completely identical except for the mutual arrangement of the terminal ethyl substituents. The ionophore molecule adopts the familiar cyclic conformation with the polar oxygen groups directed toward the interior of the molecule to wrap a metal ion and the nonpolar groups toward the exterior. The metal ion is six-coordinated in the range of 2.31 (1)–2.83 (1) Å by five oxygens of one anionic molecule and a carboxylate oxygen of its pairing molecule; the metal-metal separation is 3.197 (2) Å. This is the first crystal structure in which an exact 2-fold symmetry exists in the lasalocid A dimer. Crystallographic details for  $\text{Ag}^+(\text{C}_{34}\text{H}_{53}\text{O}_8)^-$ : space group  $C222_1$ ,  $a = 22.439$  (5) Å,  $b = 16.976$  (3) Å,  $c = 18.619$  (4) Å,  $V = 7092$  (3) Å<sup>3</sup>,  $Z = 8$ . The final discrepancy factors  $R_F$  and  $R_{wF}$  are 0.053 and 0.069, respectively, for 1832 observed reflections with  $F_o > 3\sigma(F_o)$ .

### Introduction

Since the advent<sup>1</sup> of lasalocid A (1) in 1951 as one of the first representatives of the naturally occurring ionophores, it has received much attention, especially because of its ability to transport mono-, di-, and trivalent cations across natural and artificial membranes, resulting in a large body of data on its biology<sup>2a</sup> and chemistry.<sup>2b</sup> X-ray crystallographic studies<sup>3</sup> of 13 lasalocid A

structures, including free acids,<sup>4</sup> an amine salt,<sup>5</sup> and complexes with such metals as  $\text{Na}^+$ ,<sup>6a-c</sup>  $\text{Ag}^+$ ,<sup>6d,e</sup>  $\text{Cs}^+$ ,<sup>6g</sup> and  $\text{Ba}^{2+}$ ,<sup>6f</sup> have shown that lasalocid A has a strong propensity to form dimeric structures,<sup>4c,6b-f</sup> in preference to monomeric<sup>4a,b,5,6a</sup> or polymeric<sup>6g</sup> ones; this is due to the relatively small molecular size of lasalocid A among acid ionophores that makes it difficult for a single anion to provide three-dimensional nonpolar protection for a metal ion in a 1:1 complex.<sup>3</sup> Somewhat surprisingly, of the seven dimeric



- (1) Berger, J.; Rachlin, A. I.; Scott, W. E.; Sternbach, W. E.; Goldberg, M. W. *J. Am. Chem. Soc.* **1951**, *73*, 5295-5298.  
 (2) (a) Westley, J. W. *Polyether Antibiotics: Naturally Occurring Acid Ionophores*; Marcel Dekker: New York, Basel, 1982; Vol. I. (b) *Ibid.*, Vol. II.

- (3) For reviews, see: (a) Duesler, E. N.; Paul, I. C. In ref 2b, pp 138-164. (b) Hilgenfeld, R.; Saenger, W. *Top. Curr. Chem.* **1982**, *101*, 28-37.  
 (4) (a) Friedman, J. M.; Rousseau, D. L.; Shen, C.; Chiang, C. C.; Duesler, E. N.; Paul, I. C. *J. Chem. Soc., Perkin Trans. 2* **1979**, 835-838. (b) 5-Bromo-lasalocid A ethanol solvate: Chiang, C. C.; Paul, I. C. Unpublished data in ref 3a, pp 157-158. (c) Bissell, E. C.; Paul, I. C. *J. Chem. Soc., Chem. Commun.* **1972**, 967-968.  
 (5) Westley, J. W.; Evans, R. H., Jr.; Blout, J. F. *J. Am. Chem. Soc.* **1977**, *99*, 6057-6061.  
 (6) (a) Chiang, C. C.; Paul, I. C. *Science* **1977**, *196*, 1441-1443. (b) Smith, G. D.; Duax, W. L.; Fortier, S. *J. Am. Chem. Soc.* **1978**, *100*, 6725-6727. (c) Schmidt, P. G.; Wang, A. H.-J.; Paul, I. C. *Ibid.* **1974**, *96*, 6189-6191. (d) Maier, C. A.; Paul, I. C. *J. Chem. Soc. D* **1971**, 181-182. (e) Heijja, C. I.; Duesler, E. N.; Paul, I. C. Unpublished data in ref 3a, pp 146-147. (f) Johnson, S. M.; Herrin, J.; Liu, S. J.; Paul, I. C. *J. Am. Chem. Soc.* **1970**, *92*, 4428-4435. (g) Paton, W. F.; Paul, I. C. Unpublished data in ref 3a, pp 154-155.